Propulsion and Power Research 2019;8(3):243−252

http://ppr.buaa.edu.cn/

Propulsion and Power Research

www.sciencedirect.com

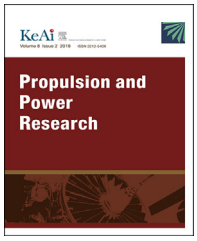

ORGINAL ARTICLE

Heat and mass transfer analysis on flow of Williamson nanofluid with thermal and velocity slips: Buongiorno model

Yap Bing Kho[a], Abid Hussanan[b,c,*], Muhammad Khairul Anuar Mohamed[a], Mohd Zuki Salleh[a]

[a]*Applied & Industrial Mathematics Research Group, Faculty of Industrial Sciences & Technology, Universiti Malaysia Pahang, Malaysia*
[b]*Division of Computational Mathematics and Engineering, Institute for Computational Science, Ton Duc Thang University, Ho Chi Minh City, Vietnam*
[c]*Faculty of Mathematics and Statistics, Ton Duc Thang University, Ho Chi Minh City, Vietnam*

Received 11 December 2017; accepted 14 January 2019
Available online 23 August 2019

KEYWORDS

Williamson nanofluid;
Slip conditions;
Heat transfer;
Stretching sheet

Abstract The thermal and velocity slips of boundary layer of Williamson nanofluid over a stretching sheet are studied numerically. Buongiorno model is used to explore the heat transfer phenomena caused by Brownian motion and thermophoresis. Using similarity transformations, the governing equations are reduced to a set of nonlinear ordinary differential equations (ODEs). These equations are solved numerically by using Shooting method. The effects of non-Newtonian Williamson parameter, velocity and thermal slip parameters, Prandtl number, Brownian parameter, Schmidt number, Lewis number, Brownian motion parameter, thermophoresis parameter on velocity, temperature and concentration fields are shown graphically and discussed. The results found that the thickness of boundary layer decreases as the slip and thermal factor parameter increases. Further, present results indicate that the nanofluid

*Corresponding author.
E-mail addresses: yapbing90@hotmail.com (Yap Bing Kho), abidhussanan@tdtu.edu.vn (Abid Hussanan), baa_khy@yahoo.com (Muhammad Khairul Anuar Mohamed), zuki@ump.edu.my (Mohd Zuki Salleh).

Peer review under responsibility of Beihang University.

Production and Hosting by Elsevier on behalf of KeAi

https://doi.org/10.1016/j.jppr.2019.01.011

temperature and concentration are enhanced with a rise of Williamson parameter. The Nusselt number is reduced with an increase of the Lewis and Prandtl numbers.

Nomenclature

a, b	positive constant for stretching rate
B	thermal slip parameter
C	nanoparticle volume fraction
C_p	effective heat capacity of nanoparticle
C_w	nanoparticle volume fraction at the sheet
C_∞	nanoparticle volume fraction far from the sheet
D_B	Brownian diffusion coefficient
D_T	thermophoresis diffusion coefficient
f	dimensionless stream function
Le	Lewis number
Nbt	diffusivity ratio parameter
Nc	heat capacities ratio parameter
Pr	Prandtl number
Re	Reynolds number
Sc	Schmidt number
Sh	Shearwood number
T	fluid temperature
T_w	temperature of fluid near sheet
T_∞	ambient temperature
u	velocity component along x direction
v	velocity component along y direction

Greek letters

α	nanofluid thermal diffusivity
θ	dimensionless temperature
ρ	density of nanofluid
ρ_p	nanoparticles density
μ	dynamic viscosity
ν	kinematic viscosity
λ	non-Newtonian Williamson parameter
δ	velocity slip parameter
ϕ	dimensionless nanoparticle volume fraction
Γ	time constant

1. Introduction

Nanofluid has been discovered and discussed by many researchers due to its unique properties and well known as the suspended colloidal liquid with nano-size metallic or non-metallic particles. Buongiorno [1] noted that the nanoparticle absolute velocity can be viewed as the sum of the base fluid velocity and a relative velocity. He considered in turn seven slip mechanisms: inertia, Brownian diffusion, thermophoresis, diffusiophoresis, Magnus effect, fluid drainage, and gravity settling. After examining each of these in turn, he concluded that in the absence of turbulent effects it is the Brownian diffusion and the thermophoresis that will be important. Adding nanoparticles to a base fluid enhances the thermal conductivity of the traditional heat transfer fluids like water, kerosene mineral oils and ethylene glycol. Thus, nanofluids can potentially be used as heat transfer fluids for cooling of electronics, vehicles engine cooling, solar water heating, nuclear reactors, heat exchanger, laser diodes, oscillating heat pipes. Corcione et al. [2] investigated nanofluids natural convection flow inside a differentially heated cavity using Buongiorno's model and found that the two phase mixture method is more accurate than the single phase model. A numerical study was conducted by Garoosi et al. [3] using Buongiorno's model. They analyzed natural and mixed convection heat transfer of a nanofluid (Al_2O_3-water) in a laterally heated square cavity. Eiamsa-ard et al. [4] study the heat transfer enhancement of TiO_2-water nanofluid in a heat exchanger tube equipped with overlapped dual twisted-tapes. Results of the following papers indicated that the thermophoresis force is important for Al_2O_3-water and specially TiO_2-water nanofluids. In fact for nanoparticles with low thermal conductivity like TiO_2, this force is very important. Some researchers like Turkyilmazoglu [5], Qasim et al. [6], Hussanan et al. [7], Swalmeh et al. [8] and Afridi et al. [9] who studied the heat transfer flow with nanofluids, stated that even in the presence of low concentration of nanoparticles, the suspensions can enhance thermal conductivity up to 20%. The enhancement of thermal conductivity mainly depends on some factors like the material of particles, shape/size of particles, temperature of the fluid material, and so on. The purpose of heat transfer coefficient is to determine the factor in forced convection cooling or heating application, like the heat exchange process involved in electrical engine systems.

In the work of Krishnamurthy et al. [10], Williamson nanofluid is categorized as visco-inelastic fluids. Blasius [11] initially studied the problem of velocity boundary layer on a flat plat followed by Sakiadis [12] who investigated the theoretical aspect of approximate and exact method for performance of boundary layer flow through a flat surface. Next, Ramesh et al. [13] had studied the convective boundary condition on Blasius and Sakiadis flows with Williamson fluid. Prior to that, Khan and Khan [14] carried

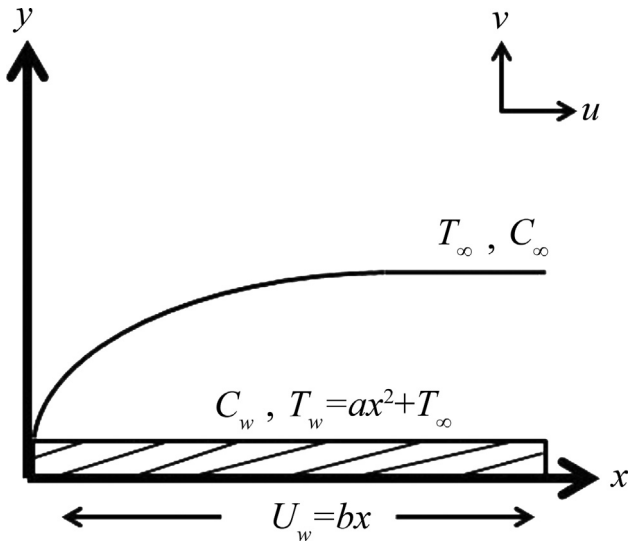

Figure 1 The physical model.

out the investigation on boundary layer flows of Williamson fluid by using homotopy analysis method (HAM). He found that the thickness of boundary layer decreases as Williamson parameter increases. Later, Nadeem and Hussain [15] analyzed the problem on Williamson nanofluid with magnetohydrodynamic (MHD) flow over a heated surface and found out that the thermal conductivity of Williamson fluid is lower than the MHD Williamson nanofluid.

Thermal energy happens when there is a temperature difference between objects. Heat transfers in non-Newtonian fluids have become common and important in some fields such as reactor cooling systems, electronic packing and so on. Kurtcebe and Erim [16] studied the problem of turbine cooling application with heat transfer in non-Newtonian visco-inelastic fluid and concluded that the upper limit of visco-inelastic parameter depends to the Reynolds number. The heat transfer analysis flow in nanofluids over a stretching sheet is important and crucial for the optimum quality of the final product especially in polymer extrusion production. Ibrahim and Shankar [17] studied the heat transfer and MHD boundary layer flow in nanofluid past over a stretching sheet. Krishnamurthy et al. [18] investigated the effect of chemical reaction on melting heat transfer and MHD boundary layer flow of Williamson nanofluid. Meanwhile, the flow features and convective heat transfer of Cu-water nanofluids were investigated by Xuan and Li [19]. According to their findings, the heat transfer feature increases as the volume fraction of nanoparticles increases. With the same Reynolds number, the suspended nanoparticles show higher heat transfer coefficient and remarkably enhance heat transfer process compared to the base fluid. Heris et al. [20] carried out the experiment on convective heat transfer laminar flow over oxide nanofluid with boundary condition of constant wall temperature. They concluded that there are several factors to enhance the heat transfer for nanofluid, as well as increase the chaotic movements of nanoparticles, thermal conductivity, interactions and fluctuations.

Table 1 Comparison of temperature gradient $-\theta'(0)$ for Prandtl number in viscous case.

Pr	Ishak et al. [26] Keller box method	Hayat et al. [27] exact solutions	Present study shooting method
0.72	0.8086	0.808631	0.808834
1	1.0000	1.000000	1.000008
3	1.9237	1.923682	1.923678
10	3.7207	3.720673	3.720671

Slip condition is considered since the presence of nanoparticles causes the interface of slip velocity between fluid and solid boundary. Yang [21] had presented the viscous flow over a solid surface with slip boundary condition. The interfacial interaction between fluid and solid is reflected by slip condition contributed by the interaction of intermolecular and roughness of wall surface. Noghrehabadi et al. [22] studied the problem of the partial slip boundary condition effect on nanofluids with prescribed wall temperature over a stretching sheet. The Nusselt and Sherwood number decreases as the velocity slip parameter increases. Malvandi et al. [23] conducted an examination on the slip effects of nanofluids in unsteady stagnation point over a stretching sheet. In their work, an increase in the values of slip parameter caused the values of skin coefficient to drop. The slip and no slip conditions on the laminar nanofluids by forced convection were numerically studied by Raisi et al. [24]. They found out that only higher Reynolds number affects the rate of heat transfer as slip velocity coefficient increases.

Motivated by above analysis, our aim is to study the slip conditions and heat transfer analysis on Williamson nanofluid over a stretching sheet is studied.

2. Mathematical formulation

This assumed that the flow of Williamson nanofluid over a stretching sheet on two-dimension is steady state and incompressible. The physical model is shown in Figure 1. The linear velocity on the sheet surface can be defined as $U_w(x) = bx$ while the b and x represent the constant and the coordinate measured along the stretching sheet respectively. y is the coordinate measured normal to stretching sheet at $y = 0$. The wall temperature as $T_w = ax^2 + T_\infty$ and the constant during the stretching surface is illustrated as the fraction of nanoparticles C_w. The nanoparticle fraction ambient values of temperature are denoted as C_∞ when y continuous tends to infinity.

The two dimensional boundary layer governing equations of non-Newtonian Williamson nanofluid flow are as follows:

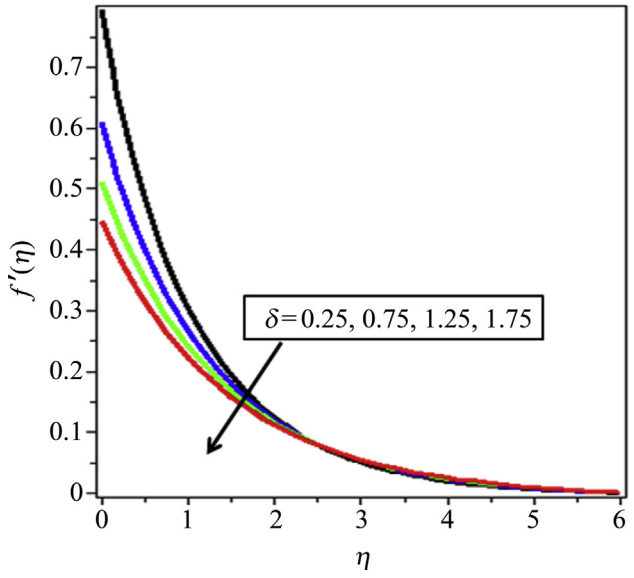

Figure 2 Velocity profiles for velocity slip parameter, when $\lambda = 0.5$, $B = 1$, $Nc = 2.5$, $Nbt = 2$, $Le = 10$, $Sc = 5$ and $Pr = 7$.

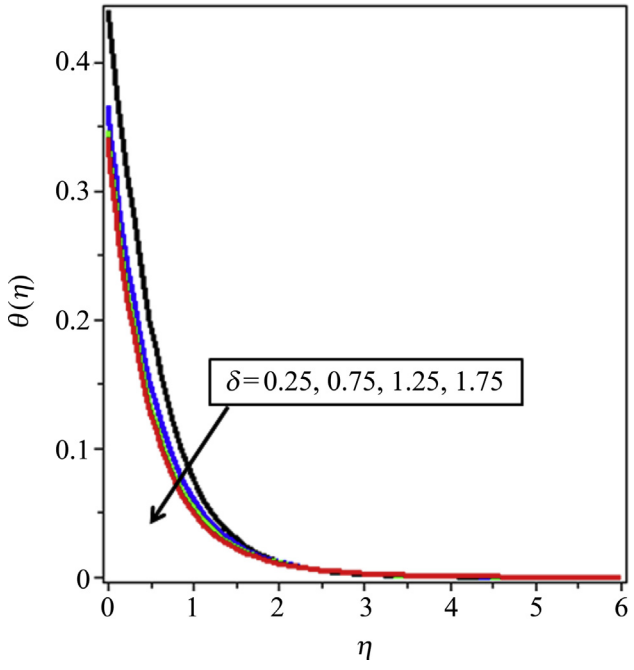

Figure 3 Temperature profiles for velocity slip parameter, when $\lambda = 0.5$, $B = 1$, $Nc = 2.5$, $Nbt = 2$, $Le = 10$, $Sc = 5$ and $Pr = 7$.

$$\frac{\partial u}{\partial x}+\frac{\partial v}{\partial y}=0 \tag{1}$$

$$u\frac{\partial u}{\partial x}+v\frac{\partial u}{\partial y}=\nu\frac{\partial^2 u}{\partial y^2}+\sqrt{2}\nu\Gamma\frac{\partial u}{\partial y}\frac{\partial^2 u}{\partial y^2} \tag{2}$$

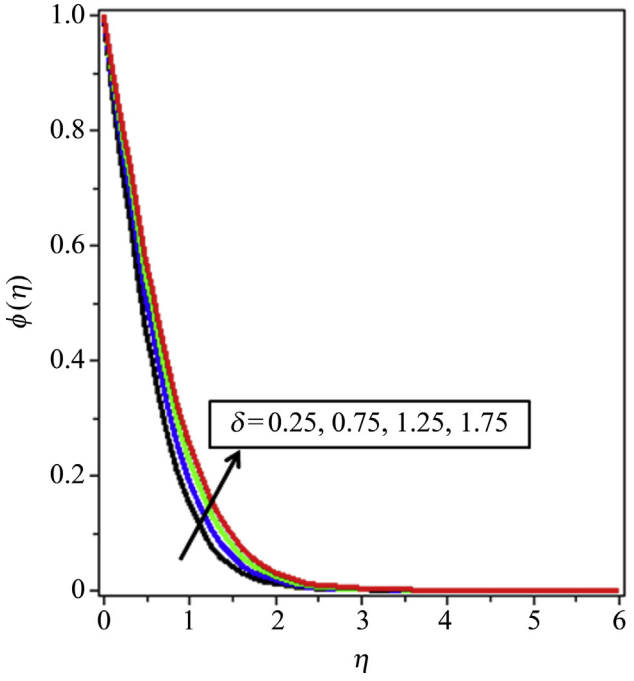

Figure 4 Concentration profiles for velocity slip parameter, when $\lambda = 0.5$, $B = 1$, $Nc = 2.5$, $Nbt = 2$, $Le = 10$, $Sc = 5$ and $Pr = 7$.

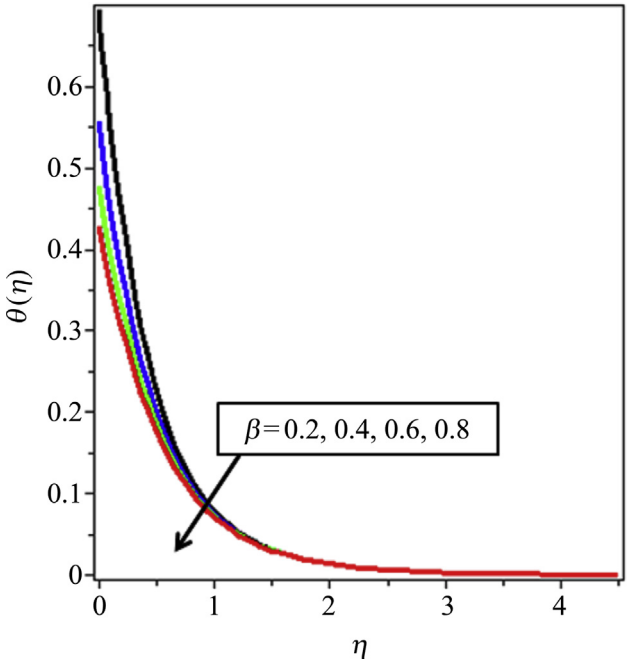

Figure 5 Temperature profiles for thermal slip parameter, when $\lambda = 0.5$, $\delta = 0.5$, $Nc = 2.5$, $Nbt = 2$, $Le = 10$, $Sc = 5$ and $Pr = 7$.

$$u\frac{\partial T}{\partial x}+v\frac{\partial T}{\partial y}=\alpha\frac{\partial^2 T}{\partial y^2}+\frac{\rho_p C_p}{\rho C}\left[D_B\frac{\partial C}{\partial y}\frac{\partial T}{\partial y}+\frac{D_T}{T_\infty}\left(\frac{\partial T}{\partial y}\right)^2\right] \tag{3}$$

$$u\frac{\partial C}{\partial x}+v\frac{\partial C}{\partial y}=D_B\frac{\partial^2 C}{\partial y^2}+\frac{D_T}{T_\infty}\frac{\partial^2 T}{\partial y^2} \tag{4}$$

Then subjected to the appropriated boundary conditions are as below:

$$u=u_w+\delta^*\mu\left(\frac{\partial u}{\partial y}\right),\ v=0,\ T=T_w+B^*\frac{\partial T}{\partial y},\ C=C_w \text{ at } y=0$$
$$u\to 0,\ T\to T_\infty,\ C=C_\infty \text{ as } y\to\infty \tag{5}$$

Following Yasin et al. [25], the similarity transformations are as below:

$$u=bxf'(\eta),\ v=-(b\nu)^{\frac{1}{2}}f(\eta),\ \eta=\sqrt{\frac{b}{\nu}}y$$
$$\theta(\eta)=\frac{T-T_\infty}{T_w-T_\infty},\ \phi(\eta)=\frac{C-C_\infty}{C_w-C_\infty} \tag{6}$$

By using similarity transformations, the ordinary differential equations are formed as follow:

$$f'''(\eta)+\lambda f''''(\eta)f''(\eta)+f''(\eta)f(\eta)-f'^2(\eta)=0 \tag{7}$$

$$\theta''(\eta)+Prf(\eta)\theta'(\eta)-2Prf'(\eta)\theta(\eta)+\frac{Nc}{Le}\theta'(\eta)\phi'(\eta)$$
$$+\frac{Nc}{(Le)(Nbt)}\theta'^2(\eta)=0 \tag{8}$$

$$\phi''(\eta)+Scf(\eta)\phi'(\eta)+\frac{1}{Nbt}\theta''(\eta)=0 \tag{9}$$

Where

$$\lambda=\sqrt{\frac{2b^3}{\nu}}\Gamma x,\ Pr=\frac{\nu}{\alpha},\ Nc=\frac{\rho_p C_p}{\rho C}(C_w-C_\infty)$$
$$Nbt=\frac{T_\infty D_B(C_w-C_\infty)}{D_T(T_w-T_\infty)},\ Le=\frac{\alpha}{D_B},\ Sc=\frac{\nu}{D_B}$$

and f, θ and ϕ are functions of η and prime denotes derivatives with respect to η. The corresponding boundary conditions take the form:

$$f(0)=0,\ f'(0)=1+\delta f''(0),\ \theta(0)=1+\beta\theta'(0),$$
$$\phi(0)=1 \text{ at } y=0$$
$$f'(\infty)=0,\ \theta(\infty)=0,$$
$$\phi(\infty)=0 \text{ as } y\to 0 \tag{10}$$

The skin friction C_f, local Nusselt number Nu and Sherwood number Sh are defined as

$$C_f=\frac{\tau_w}{\rho U_w^2},\ Nu=\frac{xq_w}{k(T_w-T_\infty)} \text{ and } Sh=\frac{xq_w}{D_B(C_w-C_\infty)} \tag{11}$$

where τ_w is the skin friction or shear stress at the surface of the plate, q_w is the heat flux from the surface and q_m is the mass flux of the nanoparticle volume fraction from the surface, and are given by

$$\tau_w=\mu\left[\frac{\partial u}{\partial y}+\frac{\Gamma}{\sqrt{2}}\left(\frac{\partial u}{\partial y}\right)^2\right],\ q_w=-k\frac{\partial T}{\partial y}_{y=0}$$

and $q_w=-D_B\frac{\partial C}{\partial y}_{y=0}$

finally, we obtain

$$C_f\sqrt{Re}=f''(0)+\frac{\lambda}{2}f''^2(0),\ \frac{Nu}{\sqrt{Re}}=-\theta'(0)$$
$$\text{and}\ \frac{Sh}{\sqrt{Re}}=-\phi'(0), \tag{12}$$

where $Re=\frac{b}{\nu}x^2$ is the Reynold's number.

3. Numerical results

The non-linear partial differential equations are solved with similarity transformations and transform to ordinary differential equations based on the given boundary conditions. After that, the derived equations are solved by using Shooting method. Thus, we may obtain unknown initial conditions $\eta=0$ by using Shooting method and assumed the initial values for boundary value problem. In this study, there is no consideration of variation in temperature, velocity and concentration where we took large infinity condition but finite value for η. We chose $\eta \geq 6$ for the considered parameters value since it is sufficient to achieve asymptotic boundary conditions for all. Based on the comparison with previous results of other researchers (in Table 1), we concluded that this technique work efficiently and the results presented here are accurate and reliable.

4. Results and discussion

This section included the graphical results for velocity, temperature and concentration profiles for the involved variables such as velocity slip parameter, thermal slip parameter, non-Newtonian, Williamson parameter, Prandtl number, heat capacities ratio parameter, diffusivity ratio parameter, Lewis number and Schmidt number. Respectively. Figures 2–4 depicted the various values of velocity slip factor parameter for velocity, temperature and concentration profile respectively. The graphical results showed that the value of velocity profiles is reducing as the velocity slip factor parameter increases. On the other hand, the wall temperature also decrease as the velocity slip factor parameter increases. However, the nanoparticles volume fraction increase as the velocity slip factor parameter increases. Figures 5 and 6 illustrated the temperature and concentration profile on thermal slip parameter. It is found that the wall temperature and volume fraction of nanoparticles decrease due to increase of thermal slip parameter. Figures 7–9 presented the several values of non-Newtonian Williamson parameter on velocity, temperature and concentration profile, respectively. The value of velocity profiles decreases and temperature and concentration profiles increase at the same time when the Williamson parameter increases. Also, the skin friction coefficient for Williamson nanofluid is getting low as the non-Newtonian Williamson

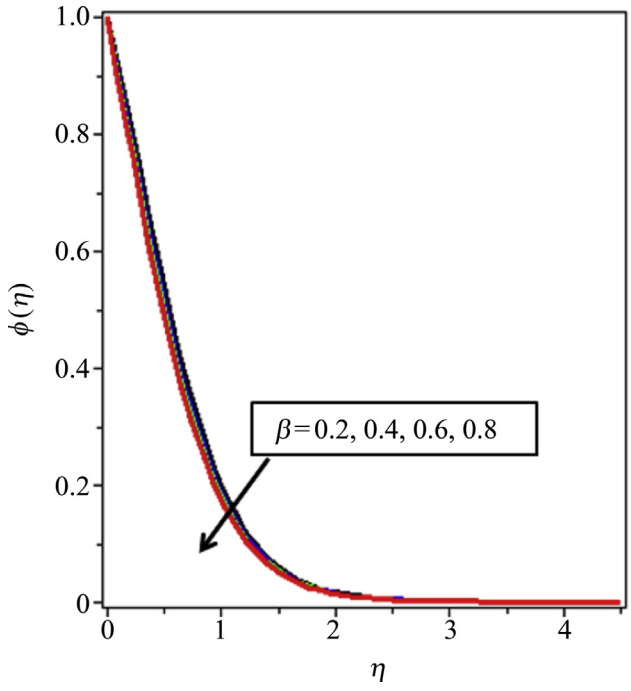

Figure 6 Concentration profiles thermal slip parameter, when $\lambda = 0.5$, $\delta = 0.5$, $Nc = 2.5$, $Nbt = 2$, $Le = 10$, $Sc = 5$ and $Pr = 7$.

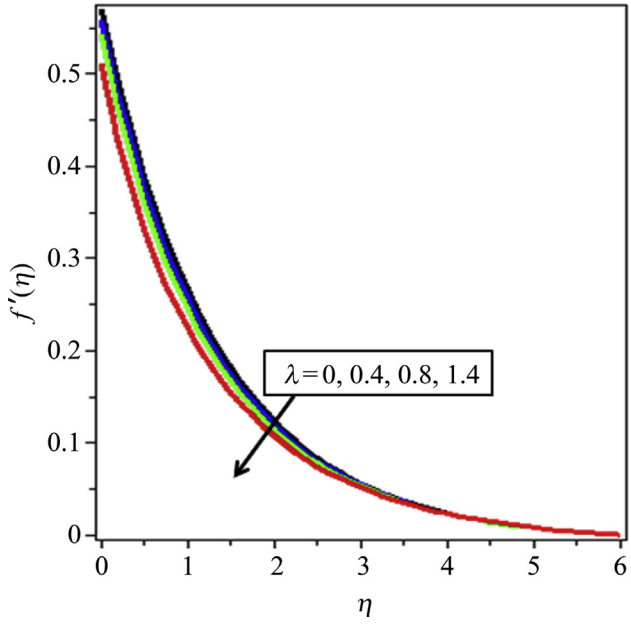

Figure 7 Velocity profiles for Williamson parameter, when $B = 0.5$, $\delta = 0.5$, $Nc = 2.5$, $Nbt = 2$, $Le = 10$, $Sc = 5$ and $Pr = 7$.

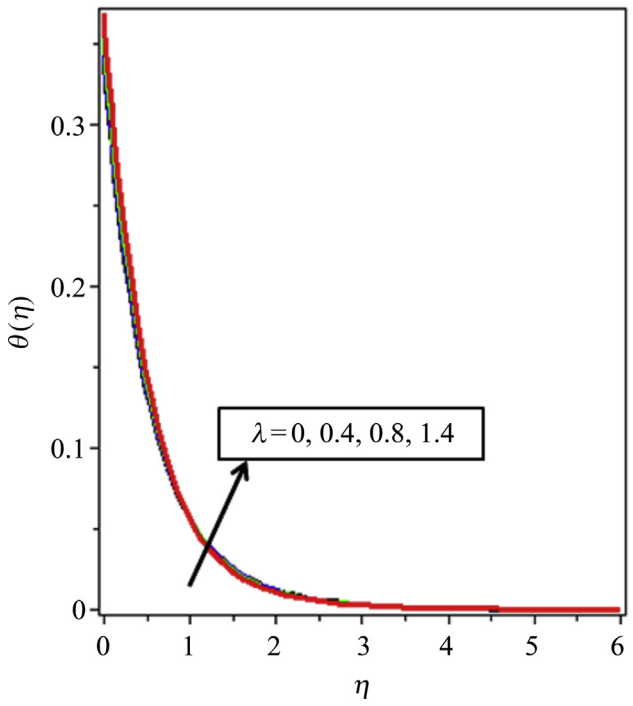

Figure 8 Temperature profiles for Williamson parameter, when $B = 0.5$, $\delta = 0.5$, $Nc = 2.5$, $Nbt = 2$, $Le = 10$, $Sc = 5$ and $Pr = 7$.

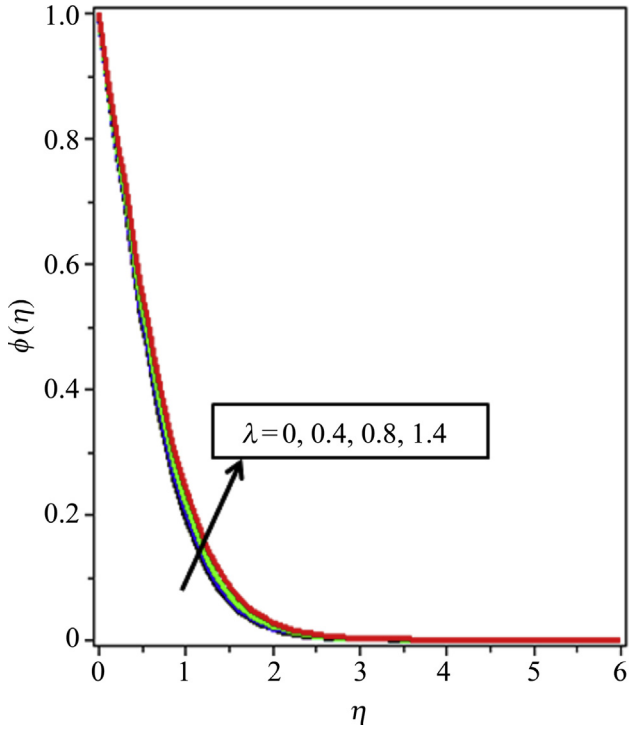

Figure 9 Concentration profiles for Williamson parameter, when $B = 0.5$, $\delta = 0.5$, $Nc = 2.5$, $Nbt = 2$, $Le = 10$, $Sc = 5$ and $Pr = 7$.

parameter increases. It is good to be used as lubricant in cooling system due to suspended nanoparticles could keep longer in the base fluids and enhance the flow characteristics of nanofluids.

Figure 10 shown that effect of Prandtl number on temperature profile. The increment of Prandtl number cause the slow rate in thermal diffusion, thus the temperature profile is reducing at all the time. Physically, it meets the logic that fluids with large Prandtl number have high viscosity and small thermal conductivity, which makes the fluid thick, and hence causes a de-crease in the velocity of the fluid.

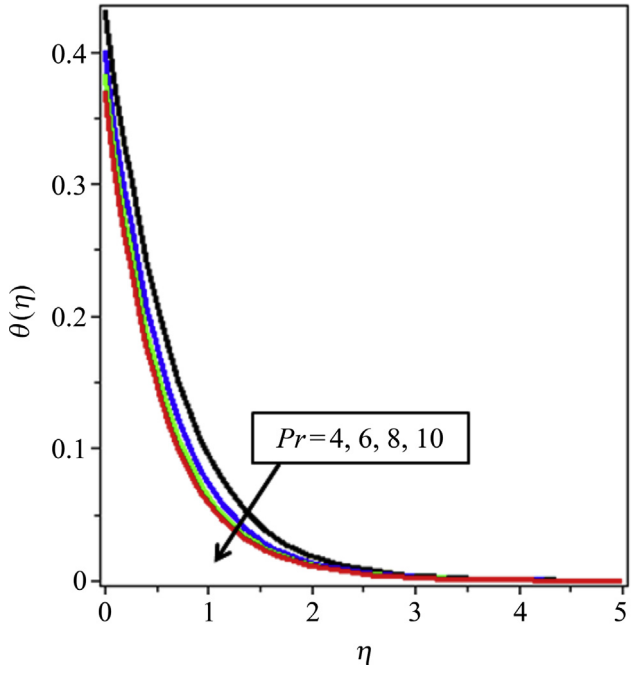

Figure 10 Temperature profiles for Prandtl number, when $\lambda = 0.5$, $B = 0.5$, $\delta = 0.5$, $Nc = 2.5$, $Nbt = 2$, $Le = 10$ and $Sc = 5$.

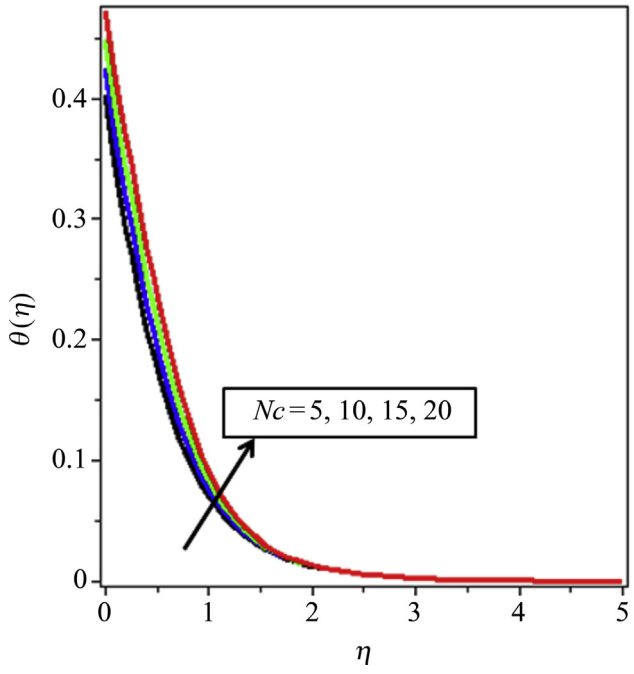

Figure 11 Temperature profiles for heat capacitance ratio parameter, when $\lambda = 0.5$, $B = 0.5$, $\delta = 0.5$, $Nbt = 2$, $Le = 10$, $Sc = 5$ and $Pr = 7$.

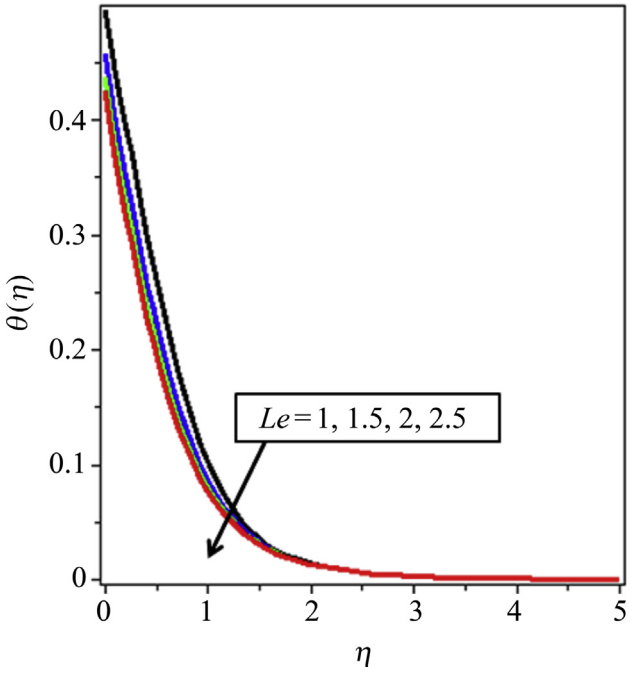

Figure 12 Temperature profiles for Lewis number, when $\lambda = 0.5$, $B = 0.5$, $\delta = 0.5$, $Nc = 2.5$, $Nbt = 2$, $Sc = 5$ and $Pr = 7$.

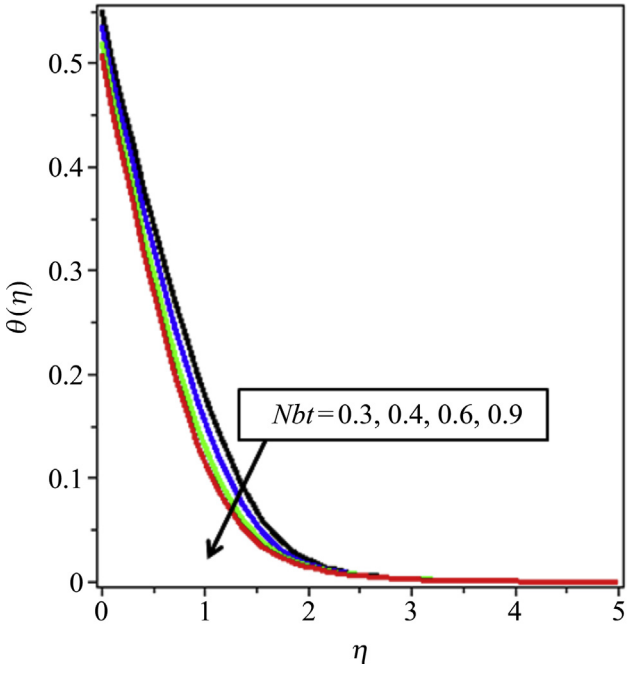

Figure 13 Temperature profiles for diffusivity ratio parameter, when $\lambda = 0.5$, $B = 0.5$, $\delta = 0.5$, $Nc = 2.5$, $Le = 10$, $Sc = 5$ and $Pr = 7$.

Figure 11 depicted the heat capacities ratio effect on temperature profile. It can be seen that the wall temperature increases when the heat capacities ratio parameter increases. Also, the boundary layer thickness decreased in this case. Therefore, the greater the value of radiation parameter, the larger the heat superficial heat flux. Figure 12 illustrated the Lewis number effects on temperature profiles. Lewis number also refer as thermal to species diffusivity ratio. Lewis number is considered for conditions where the temperature

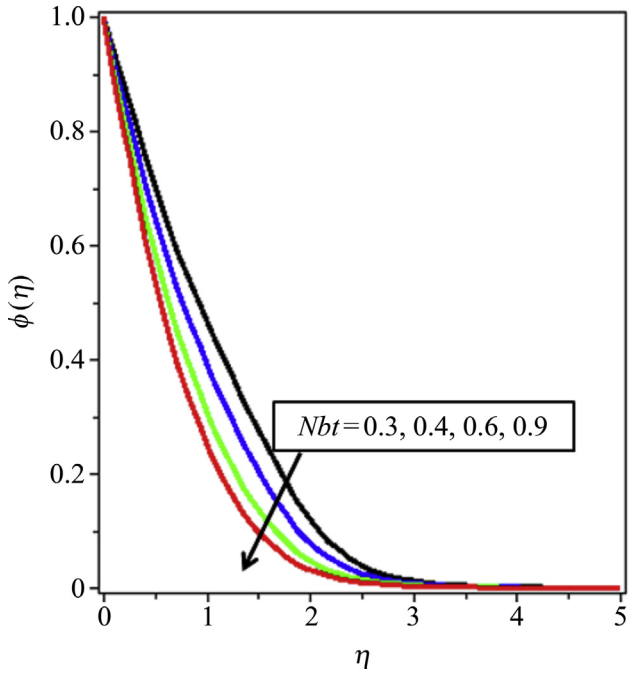

Figure 14 Concentration profiles for diffusivity ratio parameter, when $\lambda = 0.5$, $B = 0.5$, $\delta = 0.5$, $Nc = 2.5$, $Le = 10$, $Sc = 5$ and $Pr = 7$.

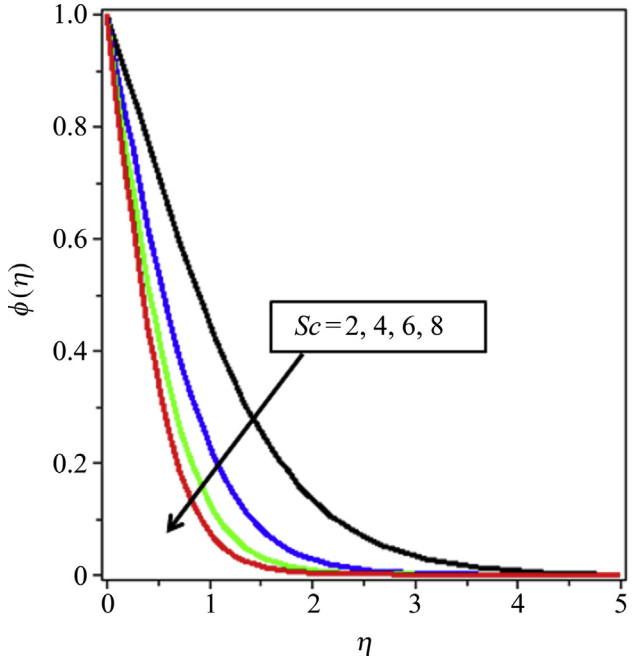

Figure 15 Temperature profiles for Schmidt number, when $\lambda = 0.5$, $B = 0.5$, $\delta = 0.5$, $Nc = 2.5$, $Nbt = 2$, $Le = 10$ and $Pr = 7$.

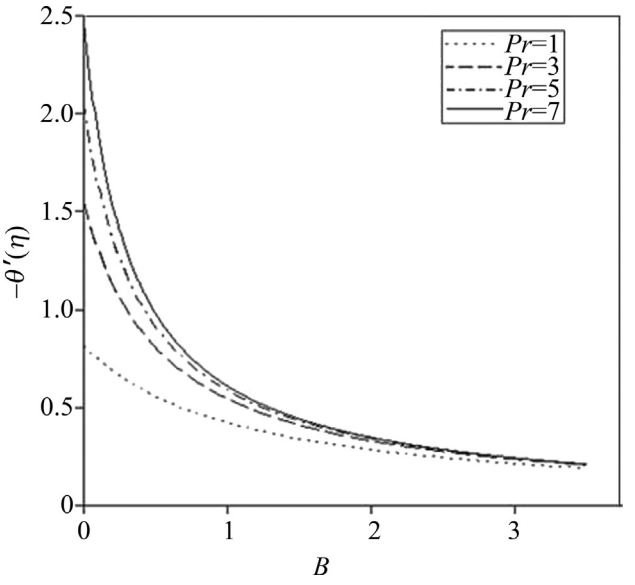

Figure 16 The effect of thermal slip parameter and Prandtl number on temperature gradient.

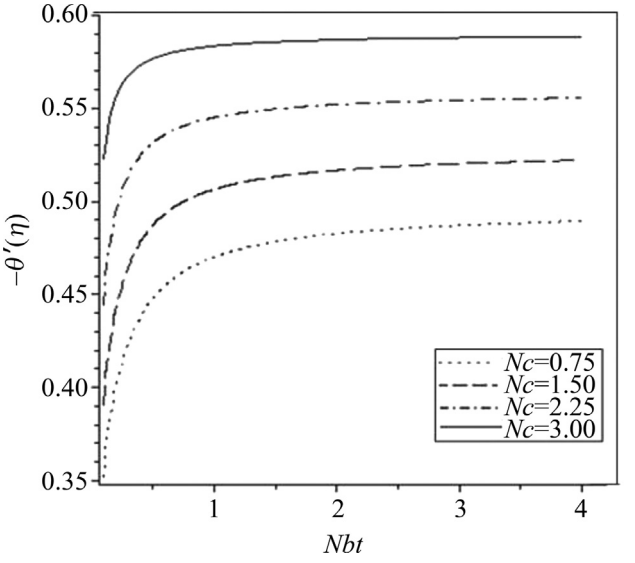

Figure 17 The effect of diffusivity ratio parameter and heat capacitance ratio parameter on temperature gradient.

and mass fraction are larger by defining temperature and diffusivities, in which reduced the convective heat transfer. Thus, the wall temperature is decreasing function against Lewis number. Figures 13 and 14 depicted the different value of diffusivity ratio parameter on temperature and concentration profiles respectively. Both the profiles dropped as the value of diffusivity ratio parameter increases. Figure 15 presented the Schmidt number on concentration profiles. The value of the profile getting less and lesser as the value of Schmidt number increases. This is because due to the momentum diffusivity effects would increase and at

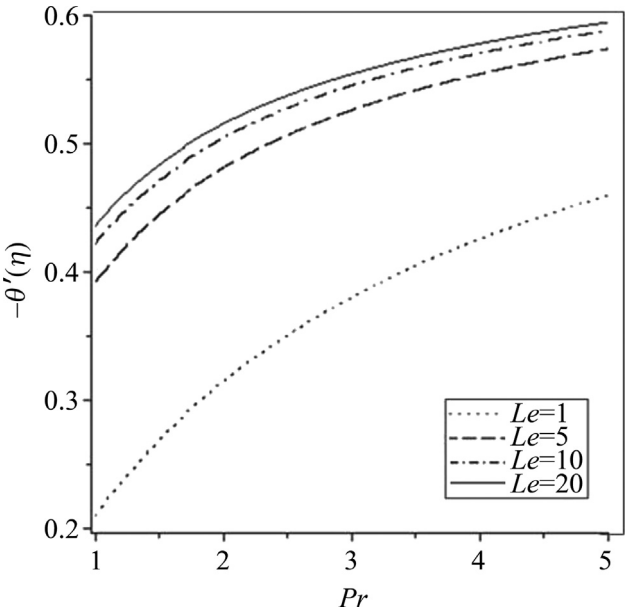

Figure 18 The effect of Lewis number and Prandtl number on temperature gradient.

the same time, it will slow down the effects of mass transfer rate leading to lower concentration profile.

Figure 16 presented the effects of thermal slip parameter and Prandtl number on temperature gradient. When the value of thermal slip parameter is small, the temperature gradient is high. However, with increasing the Prandtl number will lead the heat transfer rate decreases sharply. The effect of diffusivity ratio parameter and heat capacitance ratio parameter on temperature gradient was shown in Figure 17. Obviously the temperature gradient rises as the value of heat capacities ratio parameter and diffusivity ratio parameter increases. Figure 18 depicted the effect of Lewis number and Prandtl number on temperature gradient. Based on the diagram, the gradient of wall temperature increases when the Prandtl number and Lewis number increases. The skin friction coefficient, gradient temperature and concentration with all the parameters have been shown in Table 2.

5. Conclusions

The problem of slip conditions on heat transfer analysis and flow of Williamson nanofluid over a stretching sheet is studied numerically. The important findings are summarized as below:

Table 2 The computation results for local skin friction coefficient, local Nusselt number and local Sherwood number respectively.

δ	B	λ	Pr	Nc	Nbt	Le	Sc	$f''(0)$	$-\theta'(0)$	$-\phi'(0)$
0.25	1	0.5	7	2.5	2	10	5	−0.824627	0.560312	1.214397
0.75								−0.521313	0.634114	0.995300
1.25								−0.391317	0.653846	0.879335
1.75								−0.316124	0.659675	0.801841
0.5	0.2	0.5	7	2.5	2	10	5		1.531496	0.731268
	0.4								1.111056	0.890411
	0.6								0.871426	0.981179
	0.8								0.716725	1.039801
1	1	0	5	2.5	2	10	5	−0.430631	0.653863	0.952791
		0.4						−0.442676	0.648285	0.935371
		0.8						−0.457476	0.641978	0.914200
		1.4						−0.489301	0.631466	0.869951
0.5	1	0.5	4	2.5	2	10	5		0.593771	
			6						0.632611	
			8						0.656798	
			10						0.673705	
0.5	1	0.5	7	5	2	10	5		0.634617	
				10					0.611296	
				15					0.587304	
				20					0.563051	
0.5	1	0.5	7	2.5	0.3	10	5		0.479166	0.251699
					0.4				0.494843	0.446998
					0.6				0.512197	0.658669
					0.9				0.524636	0.811730
0.5	1	0.5	7	2.5	2	1	5		0.538971	
						1.5			0.579227	
						2			0.599359	
						2.5			0.611296	
0.5	1	0.5	7	2.5	2	10	2			0.409463
							4			0.780050
							6			1.062968
							8			1.299821

- The results indicate that the nanofluid temperature and concentration are enhanced with a rise of Williamson parameter.
- An increase in the velocity slip parameter leads to increase in the nanoparticles volume fraction
- The higher the non-Newtonian Williamson parameter, the greater the thickness of boundary layer.
- The temperature profile was reducing at all the time and caused by increment of Prandtl number.
- An increase of velocity slip parameter would lead to an increase in the heat transfer rate.
- The wall temperature would increase when the heat capacities ratio parameter increased while temperature gradient decreases if increased in diffusivity ratio parameter.
- Temperature gradient is reduced with an increase of the Lewis and Prandtl numbers.
- An increase in thermal slip parameter would cause a drop in the temperature gradient.
- Williamson nanofluid has lower skin friction coefficient when the non-Newtonian Williamson parameter increased.

Acknowledgements

The authors gratefully acknowledge the financial supports received from Ministry of Higher Education, University Malaysia Pahang (UMP), Malaysia, through vote number RDU 150101 and RDU 170358. The second author would like to acknowledge Ton Duc Thang University, Ho Chi Minh City, Vietnam for the financial support.

References

[1] J. Buongiorno, Convective transport in nanofluids, ASME Journal of Heat Transfer 128 (2006) 240−250.
[2] M. Corcione, M. Cianfrini, A. Quintino, Two-phase mixture modeling of natural convection of nanofluids with temperature-dependent properties, Int. J. Therm. Sci. 71 (2013) 182−195.
[3] F. Garoosi, S. Garoosi, K. Hooman, Numerical simulation of natural convection and mixed convection of the nanofluid in a square cavity using Buongiorno model, Powder Technol. 268 (2014) 279−292.
[4] S. Eiamsa-ard, K. Kiatkittipong, W. Jedsadaratanachai, Heat transfer enhancement of TiO_2/water nanofluid in a heat exchanger tube equipped with overlapped dual twisted-tapes, Eng. Sci. Technol., Int. J. 18 (2015) 336−350.
[5] M. Turkyilmazoglu, Exact analytical solutions for heat and mass transfer of MHD slip flow in nanofluids, Chem. Eng. Sci. 84 (2012) 182−187.
[6] M. Qasim, Z.H. Khan, R.J. Lopez, W.A. Khan, Heat and mass transfer in nanofluid thin film over an unsteady stretching sheet using Buongiorno's model, The European Physical Journal Plus 131 (2016) 1−11.
[7] A. Hussanan, M.Z. Salleh, I. Khan, Microstructure and inertial characteristics of a magnetite ferrofluid over a stretching/shrinking sheet using effective thermal conductivity model, J. Mol. Liq. 255 (2018) 64−75.
[8] M.Z. Swalmeh, H.T. Alkasasbeh, A. Hussanan, M. Mamat, Heat transfer flow of Cu-water and Al_2O_3-water micropolar nanofluids about a solid sphere in the presence of natural convection using Keller-box method, Results in Physics 9 (2018) 717−724.
[9] M.I. Afridi, M. Qasim, S. Saleem, Second law analysis of three dimensional dissipative flow of hybrid nanofluid, J. Nanofluids 7 (2018) 1272−1280.
[10] M.R. Krishnamurthy, B.J. Gireesha, B.C. Prasannakumara, R.S.R. Gorla, Thermal radiation and chemical reaction effects on boundary layer slip flow and melting heat transfer of nanofluid induced by a nonlinear stretching sheet, Nonlinear Eng. 5 (3) (2016) 147−159.
[11] H. Blasius, The Boundary Layers in Fluids with Little Friction, 1950.
[12] B.C. Sakiadis, Boundary layer behavior on continuous solid surfaces, I: boundary-layer equations for two-dimensional and axisymmetric flow, AIChE J. 7 (1) (1961) 26−28.
[13] G.K. Ramesh, B.J. Gireesha, R.S.R. Gorla, Study on Sakiadis and Blasius flows of Williamson fluid with convective boundary condition, Nonlinear Eng. 4 (4) (2015) 215−221.
[14] N.A. Khan, H. Khan, A boundary layer flows of non-Newtonian Williamson fluid, Nonlinear Engineering Nonlinear Engineering 3 (2) (2014) 107−115.
[15] S. Nadeem, S.T. Hussain, Analysis of MHD Williamson nano fluid flow over a heated surface, J. Appl. Fluid Mech. 9 (2) (2016) 729−739.
[16] C. Kurtcebe, M.Z. Erim, Heat transfer of non-Newtonian viscoinelastic fluid in an axisymmetric channel with a porous wall for turbine cooling application, Int. Commun. Heat Mass Transf. 29 (7) (2002) 971−982.
[17] W. Ibrahim, B. Shankar, MHD boundary layer flow and heat transfer of a nanofluid past a permeable stretching sheet with velocity, thermal and solutal slip boundary conditions, Comput. Fluids 75 (2013) 1−10.
[18] M.R. Krishnamurthy, B.C. Prasannakumara, B.J. Gireesha, R.S.R. Gorla, Effect of chemical reaction on MHD boundary layer flow and melting heat transfer of Williamson nanofluid in porous medium, Eng. Sci. Technol., Int. J. 19 (1) (2016) 53−61.
[19] Y. Xuan, Q. Li, Investigation on convective heat transfer and flow features of nanofluids, J. Heat Transf. 125 (1) (2003) 151−155.
[20] S.Z. Heris, S.G. Etemad, M.N. Esfahany, Experimental investigation of oxide nanofluids laminar flow convective heat transfer, Int. Commun. Heat Mass Transf. 33 (4) (2006) 529−535.
[21] F. Yang, Slip boundary condition for viscous flow over solid surfaces, Chem. Eng. Commun. 197 (4) (2009) 544−550.
[22] A. Noghrehabadi, R. Pourrajab, M. Ghalambaz, Effect of partial slip boundary condition on the flow and heat transfer of nanofluids past stretching sheet prescribed constant wall temperature, Int. J. Therm. Sci. 54 (2012) 253−261.
[23] A. Malvandi, F. Hedayati, D.D. Ganji, Slip effects on unsteady stagnation point flow of a nanofluid over a stretching sheet, Powder Technol. 253 (2014) 377−384.
[24] A. Raisi, B. Ghasemi, S.M. Aminossadati, A numerical study on the forced convection of laminar nanofluid in a microchannel with both slip and no-slip conditions, Numer. Heat Transf., Part A: Applications 59 (2) (2011) 114−129.
[25] M.H. Yasin, A. Ishak, I. Pop, MHD heat and mass transfer flow over a permeable stretching/shrinking sheet with radiation effect, J. Magn. Magn. Mater. 407 (2016) 235−240.
[26] A. Ishak, R. Nazar, I. Pop, Heat transfer over an unsteady stretching permeable surface with prescribed wall temperature, Nonlinear Anal. Real World Appl. 10 (5) (2009) 2909−2913.
[27] T. Hayat, Z. Abbas, T. Javed, Mixed convection flow of a micropolar fluid over a non-linearly stretching sheet, Phys. Lett. A 372 (5) (2008) 637−647.